ELSEVIER

Biochimica et Biophysica Acta 1230 (1995) 97–113

BBA Biochimica et Biophysica Acta

Absorption and ADMR studies on bacterial photosynthetic reaction centres with modified pigments

G. Hartwich [a], H. Scheer [a], V. Aust [b], A. Angerhofer [b,*]

[a] *Botanisches Institut, Universität München, Menzinger Str. 67, D-80638 München, Germany*
[b] *3. Physikalisches Institut, Universität Stuttgart, D-70550 Stuttgart, Germany*

Received 19 October 1994; revised 13 February 1995; accepted 8 March 1995

Abstract

[3-Vinyl]-13^2-OH-bacteriochlorophyll *a* has been selectively exchanged against native bacteriochlorophyll *a* in the monomer binding sites at the A- and B-branch of the photosynthetic reaction centre from *Rhodobacter sphaeroides*. Optical absorption and absorption-detected magnetic resonance experiments were performed on these samples at 8 K. The site-specific interaction of only pigment B_B (at the electron transfer-inactive branch) with the triplet state on the neighbouring carotenoid, spheroidene, clearly demonstrates the selective pigment exchange. The absorption spectra allow a distinction of the two monomer bacteriochlorophyll pigments (native as well as modified bacteriochlorophylls) by their absorption band maximum positions in native reaction centres: B_A absorbs at 803 nm, B_B at 812 nm. The upper exciton component of the primary donor was observed around 807 nm. The microwave induced absorption spectra of the primary donor triplet in the modified preparations are quite distinct from those of native reaction centres revealing specific pigment–pigment interactions between the monomers and the primary donor triplet state. These interactions appear as band shifts of the Q_y-transitions of the accessory monomers, and are in agreement with a primary donor triplet that is delocalized over both dimer parts.

Keywords: Photosynthesis; Reaction center; Pigment modification; [3-Vinyl]-13^2-OH-bacteriochlorophyll *a*; Triplet state; Absorption detected magnetic resonance; ADMR ; (*Rhodobacter sphaeroides*)

1. Introduction

Reaction centres (RC) of the purple photosynthetic bacterium *Rhodobacter (Rb.) sphaeroides* R26 contain four bacteriochlorophyll *a* (BChl *a*) and two bacteriopheophytin *a* (BPh *a*) molecules [1,2] in a protein complex comprised of 3 polypeptides traditionally labeled L, M, and H [3,4]. Their molecular structure has been revealed by single crystal X-ray crystallography [5–7]. The primary donor consists of a dimer of BChl *a* molecules, the so-called 'special pair' [8]. The remaining two BChl and two BPh molecules are lined up in two 'branches' on either side of the dimer, labelled A and B. Although the pigments on these two branches and the L- and M-subunits are related to each other by an approximate C_2 symmetry, the axis of which runs through the dimer, only branch A is active in primary light-induced electron transport [9–12]. The distinction between both pigment branches is based on small spectroscopic differences between the two BPh molecules at low temperatures which can be related to the crystal structure by the polarization of their optical transition moments in single crystals [13].

Besides the basic structural information obtained from the crystal structure, well defined modifications of the RC have been very useful in the past to investigate the structure-function relationship of the different RC components. Especially site-directed mutagenesis and exchange of cofactors have been used to study the intricate interactions between pigments and protein environment, and between

Abbreviations: ADMR, absorption detected magnetic resonance; $B_{A,B}$, accessory monomers on A- and B-branch; BChl, bacteriochlorophyll; BPhe, bacteriopheophytin; Car, carotenoid; DAD-HPLC, diode-array detected high performance liquid chromatography; DEAE, diethylaminoethylcellulose; EIRS, environmentally induced red shift; EPR, electron paramagnetic resonance; LD-ADMR, linear dichroism detected ADMR; LDAO, lauryl-dimethyl-amineoxide; LD-MIA, linear dichroism detected MIA; MIA, microwave induced absorption; *A*, absorbance; P_{870}, primary donor 'special pair'; RC, reaction centre; TL-buffer, 10 mM Tris-HCl (pH 7.5), containing 0.08% LDAO; T − S: triplet-minus-singlet

* Corresponding author. (Present address) Department of Chemistry, University of Florida, Gainesville, FL 32611, USA. Fax: +1 (904) 3920872.

SSDI 0005-2728(95)00038-0

the pigments themselves [14–19]. Using this approach, fine-tuning of such parameters as pigment excited state energy and redox potentials are possible, and specific binding pockets of the RC protein can be studied selectively [20,21].

Recently, the exchange of the BChl *a* and BPh *a* monomer pigments $B_{A,B}$ and $H_{A,B}$ with pigments modified at the 3-acetyl group has been reported [18,22]. In carotenoid-free RCs the affinity of BChl *a* to the two monomer sites A and B seems to be slightly different, making it somewhat easier to exchange B_B [22]. RCs of wild-type *Rb. sphaeroides* 2.4.1 can only be modified up to 50% of the total monomer BChl content. The exchange of pigments takes place exclusively at the B_A-site, demonstrating that the carotenoid present in these RCs effectively shields the B_B binding pocket (vide infra and [23]).

We have further explored this protective effect of the carotenoid to prepare RCs in which a modified BChl *a* containing a 3-vinyl instead of the 3-acetyl group was introduced selectively at B_A or B_B. Starting from wild-type RCs, B_A was exchanged selectively. Starting from carotenoid-deficient RCs from the mutant R26, both B_A and B_B were exchanged in a first step, followed by introduction of spheroidene, and finally re-exchange of natural BChl *a* into site B_A only. Thus, a sample was obtained which contained the modified pigment at B_B. We report on the preparation of RCs from *Rb. sphaeroides* selectively modified at either one (B_A or B_B) or both monomer BChl positions with [3-vinyl]-13^2-OH-BChl *a* in which the 3-acetyl-substituent of BChl *a* has been replaced by a vinyl group. Using low temperature absorption and absorption detected magnetic resonance at 8 K, we were able to distinguish the optical absorption bands of both monomers, and to observe distinct interactions between both monomer BChl pigments and the primary donor in its lowest excited triplet state, as well as between B_B and the carotenoid triplet state.

2. Materials and methods

2.1. Sample preparation

RCs of *Rb. sphaeroides* R26 (sample A) or wild-type strain 2.4.1 (sample B) were isolated as described elsewhere [23–25]. [3-Vinyl]-13^2-OH-BChl *a* was prepared from BChl *a* by reduction of the 3-acetyl group with $NaBH_4$ to 3-α-OH-ethyl and subsequent dehydration in pyridine to [3-vinyl]-BChl *a*. Hydroxylation at the 13^2-position occurs when [3-vinyl]-BChl is dissolved in methanol and kept in the dark for several days at 4° C in the presence of air [26].

Simultaneous exchange of BChl at the sites B_A and B_B against [3-vinyl]-13^2-OH-BChl *a* is possible by treating R26 RCs (A/cm = 1 at 865 nm), dissolved in TL-buffer (10 mM Tris, 0.08% LDAO, at pH 8) with a 10-fold molar excess of [3-vinyl]-13^2-OH-BChl *a* in methanolic solution for 90 min at 43° C. The organic solvent should not exceed 10% of the whole reaction volume in order to avoid extensive loss of RCs during the treatment by irreversible denaturation. Purification of exchanged RCs from extra pigment and denatured protein is done on DEAE-cellulose. The overall exchange rate was determined by pigment extraction and subsequent DAD-HPLC [19,27]. Repeating the whole exchange experiment one or two times leads to nearly quantitative replacement of native monomeric BChl. In the actual $B_{A,B}$-exchanged sample (sample D prior to reconstitution with spheroidene) approx. 95 ± 3% of the native monomeric BChl is replaced.

For introduction of spheroidene in carotenoidless RC, it is dissolved to maximum concentration in diethyl ether and then diluted with 3 parts (v/v) methanol. This mixture was added to the RCs (A/cm = 1 at 865 nm) to a final concentration of organic solvent of 10%. The reaction time is only 50 min at 43° C, by which about 90% of the RCs are reconstituted with the carotenoid (according to DAD-HPLC analysis). The carotenoid-reconstituted RCs of *Rb. sphaeroides* R26 without prior BChl exchange (sample C) have a spheroidene content of 87% (compared to the wild-type 2.4.1 RCs, and estimated from room temperature integral absorption at 505 nm relative to the integral primary donor absorption at 865 nm). In the $B_{A,B}$-exchanged sample (sample D), spheroidene is reconstituted to 93%.

For a substitution of BChl against [3-vinyl]-13^2-OH-BChl *a* at the B_B site only, the starting material is the $B_{A,B}$-exchanged sample. After reconstitution with spheroidene (sample D), the B_B pocket is blocked by the presence of the carotenoid (vide infra). Using the same exchange procedures as described above, but adding the native BChl *a* as the exogenous pigment and raising the temperature to 48° C, re-exchange of BChl *a* into the B_A pocket takes place (sample E). The increase in temperature is necessary because of the increased stability of carotenoid containing RCs. As a 'pleasant side effect' all RCs that are not reconstituted with spheroidene are destroyed during this treatment. In the actual B_B-replaced sample (E), at least 95% of the RCs carry [3-vinyl]-13^2-OH-BChl *a* in the B_B site. The total exchange rate at the monomeric sites is 58 ± 3%. Therefore, about 21% of the RCs in sample E still carry this pigment at the B_A site due to incomplete reverse exchange. The carotenoid content is 110% [1].

Selective BChl exchange at the B_A-site only is achieved in wild-type RCs of the strain 2.4.1. They naturally contain spheroidene close to the B_B monomer which blocks the exchange there. The procedure is the same as in the case of the re-exchange of native BChl into sample D (see above).

[1] A value exceeding 100% is possible, since the carotenoid content is normalized to that of wild-type RCs which may show a loss of their carotenoids of up to 20% during the preparation.

Table 1
Sample preparations used in this study

Sample	B_A	B_B	Carotenoid
A	BChl *a*	BChl *a*	–
B	BChl *a*	BChl *a*	native
C	BChl *a*	BChl *a*	reconstituted
D	vinyl-BChl *a*	vinyl-BChl *a*	reconstituted
E	BChl *a*	vinyl-BChl *a*	reconstituted
F	vinyl-BChl *a*	BChl *a*	native

The carotenoid present is always spheroidene, either naturally by using the wild-type strain or by reconstitution into the mutant strain R26. Vinyl-BChl *a*, abbreviation for [3-vinyl]-13^2-OH-BChl *a*.

The exchange rate of the B_A-exchanged sample F is approx. 47% of the monomeric BChl, corresponding to 94% replacement at B_A. The carotenoid content is 98%.

The high exchange rates at the B_B-site in samples D and E are especially well observed in the carotenoid triplet MIA spectra, which can be used to judge the degree of monomer exchange (see Discussion, part 4.3).

All RC preparations with exchanged pigments show the normal primary donor bleaching when exposed to actinic light. The CD spectra show no detectable structural changes besides spectral shifts due to the different absorption bands of the exchanged pigments. The different samples used in this study together with their associated letters are summarized in Table 1.

2.2. Spectroscopic methods

Our ADMR set-up has been described previously [28,29]. Linear dichroism detected ADMR (LD-ADMR) was performed as described in [30,31]. Absorption spectra at low temperatures were recorded using the optical path of the ADMR spectrometer as a single-beam absorption spectrometer in transmission mode. Absorption was calculated from transmission, using the lamp spectrum as a reference.

3. Results

The absorption spectra of the different samples under investigation, taken at 8 K, are shown in Fig. 1. The exact band locations and relative intensities of their absorption maxima are given in Table 2. The sample labels (A through F) used in the spectra and detailed in the legend of Fig. 1 are kept throughout the paper. Generally, the samples will only be referred to by these labels.

The spectra of samples A and B show the well known absorption bands of *Rb. sphaeroides* R26 and wild-type 2.4.1, respectively. Except for the carotenoid bands at 472 and 505 nm which are missing in sample A, they are almost identical. In the Q_x region, BPhe absorbs at 534 and 546 nm (pigments H_B and H_A, respectively), and BChl at 597 nm with a slight shoulder at 605 nm. The Q_y band of BPhe at 762 nm shows a shoulder at its blue side (750 nm), whereas the Q_y peak of monomeric BChl at 804 nm has a shoulder to the red (812 nm), which is somewhat more pronounced in the case of the wild-type sample B. The primary donor bands P_ of both samples appear at 895 and 893 nm, the negligible difference probably being due to slightly different detergent concentrations, or freezing conditions.

In sample C, RCs of *Rb. sphaeroides* R26 had been reconstituted with spheroidene to give 'artificial' wild-type RCs. Compared to the corresponding spectrum of B only little changes are observed. The BChl Q_x and the monomer Q_y bands are mostly affected, becoming slightly better resolved in sample C. The small red-shift of the P_ band

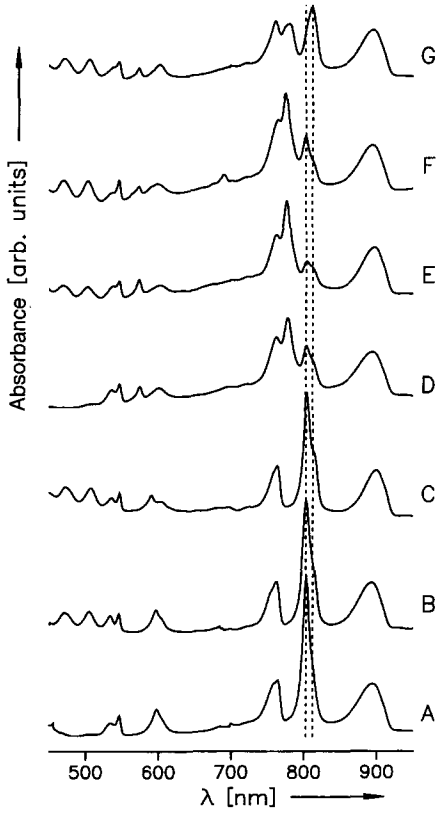

Fig. 1. Absorption spectra of RCs from *Rb. sphaeroides* at 8 K between 500 and 950 nm. All spectra were normalized to equal height at the red-most absorption band. The spectral position of the two accessory monomer pigments (803 and 812 nm) is indicated with dashed lines. The notation for the different samples in this and the following figures is as follows: (A) Untreated RCs from *Rb. sphaeroides* R26 (carotenoid-free). (B) Untreated RCs of *Rb. sphaeroides* 2.4.1 (wild-type). (C) RCs of *Rb. sphaeroides* R26, reconstituted with spheroidene. (D) RCs of *Rb. sphaeroides* R26 with both monomers (sites $B_{A,B}$) exchanged by [3-vinyl]-13^2-OH-BChl *a* and subsequently reconstituted with spheroidene. Degree of monomer exchange 95%. (E) RCs of *Rb. sphaeroides* R26 with both monomers (sites $B_{A,B}$) exchanged by [3-vinyl]-13^2-OH-BChl *a*, then reconstituted with spheroidene, and finally the monomer at site B_A re-exchanged with native BChl *a*. Degree of monomer exchange 58% (approx. 100% of B_B and still 20% of B_A). (F) RCs of *Rb. sphaeroides* 2.4.1 (wild-type) with the monomer at site B_A exchanged by [3-vinyl]-13^2-OH-BChl *a*. Degree of monomer exchange 47%.

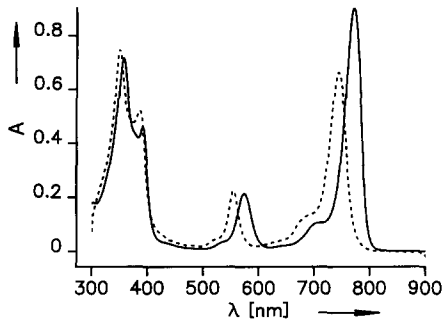

Fig. 2. Absorption spectra of BChl *a* (–) and [3-vinyl]-13^2-OH-BChl *a* (– – –) in diethyl ether at ambient temperature.

(899 nm), compared to samples A and B may again be due to slightly different solvent conditions of the sample, as above.

In samples, D, E, and F, native BChl is replaced by [3-vinyl]-13^2-OH-BChl *a*, the Q_y and Q_x bands of which appear blue shifted by about 28 and 19 nm, respectively, compared with native BChl *a* in organic solvents (Fig. 2). The environmentally induced red-shift (EIRS) which shifts the monomer Q_y bands in the RC protein to the red as compared to organic solution is the same for both pigments, i.e., the differences in peak wavelengths in vitro is conserved in the protein [19]. This is seen by the appearance of new bands in the BChl Q_x and Q_y region due to the blue-shifted absorption bands of the modified pigments.

Spectrum 1D (i.e., Fig. 1, sample D) is the absorption of a sample in which initially both monomers B_A and B_B had been replaced by the modified pigment, and then spheroidene reconstituted. At 573 and 777 nm the [3-vinyl]-13^2-OH-BChl absorption bands appear (Q_x and Q_y, respectively), and at 469 and 503 nm, similar to wild-type RCs (sample B), the spheroidene bands. The decrease of the Q_y peak of monomeric BChl at 804 nm together with HPLC data indicate an almost complete exchange. The remaining BChl *a* bands at 603 nm and around 807 nm are therefore mainly due to primary donor absorption.

Using as starting material sample D, the monomer on the electron-transfer active A-branch (L-side of the RC protein), not protected by the carotenoid, was re-exchanged selectively with the original BChl (BChl *a*) to give sample E. These RCs are expected to carry the modified pigment only at the B_B site, with a small fraction of RCs composed as in sample D due to incomplete back exchange (see Section 2). Compared to sample D we therefore observe an increase of absorbance at 803 and 599 nm; this is concurrent with a decrease and shift of the [3-vinyl]-13^2-OH-BChl absorption bands at 775 and 573 nm.

Finally, sample F represents the modification at the B_A site of *Rb. sphaeroides* wild-type 2.4.1. The bands of the modified pigments appear at 777 and 573 nm (Q_y and Q_x, respectively), and those of the remaining native monomer BChl at 812 and 602 nm. By comparison with spectrum 1E, where the B_B site monomer was modified, we can assign the Q_y band at 803 nm to B_A, and that at 812 nm to B_B. Different spectral positions are also seen for the Q_y bands of the substituted pigment, [3-vinyl]-13^2-OH-BChl. In the B_A-site it absorbs at 777 nm, in the B_B-site at 775 nm. The Q_x absorption bands of the modified pigments appear at 573 nm.

Fig. 3 shows the 'light-minus-dark' absorption difference spectra of the RC preparations with modified pigments (samples D–F) together with that of non-modified RCs from *Rb. sphaeroides* R26 (sample A). All four spectra exhibit their primary donor bleaching band around 896 nm. Between 750 and 820 nm, a number of strong features are observed.

The 'light-minus-dark' difference spectrum of the green R26 mutant with a strong bleaching at 803 nm (with a shoulder at 810 nm) and enhanced absorption at 794 and 767 nm is well known from the literature [3,32].

The fully modified preparation (sample D) shows

Table 2
Spectral positions of the absorption maxima and positive (+) and negative (–) MIA bands in Figs. 1 and 5 in nm with relative intensities (in parentheses) normalized to the primary donor absorption (absorption spectra, Fig. 1) and primary donor bleaching ($^3P_{870}$ MIA spectra, Fig. 5)

Sample	Absorption [nm]	MIA [nm]
A	535 (29), 547 (37), 598 (49), 760^S (101), 765 (106), 803 (306), 895 (100)	470$^-$, 605$^-$, 659$^-$, 754$^+$, 764$^+$, 774$^+$, 798$^+$, 802$^-$, 807$^+$, 814$^-$, 820$^+$, 896$^-$
B	472 (39), 505 (41), 534 (33), 546 (37), 597 (44), 605^S (27), 750^S (73), 762 (102), 804 (268), 812^S (132), 893 (100)	473$^-$, 604$^-$, 658$^-$, 754$^+$, 765$^{S,+}$, 773$^+$, 797$^+$, 802$^-$, 809$^+$, 815$^-$, 820$^+$, 896$^-$
C	473 (64), 507 (62), 536^S (40), 547 (50), 591 (46), 604^S (32), 764 (110), 804 (272), 812^S (134), 899 (100)	473$^-$, 604$^-$, 658$^-$, 753$^+$, 765$^+$, 774$^+$, 798$^+$, 804$^-$, 809$^+$, 815$^-$, 821$^+$, 901$^-$
D	469 (28), 503 (24), 538 (26), 546 (36), 573 (40), 603 (28), 762 (127), 777 (201), 805 (71), 812^S (59), 897 (100)	603$^-$, 658$^-$, 725$^-$, 779$^+$, 790$^-$, 802$^+$, 809$^-$, 818$^+$, 898$^-$
E	469 (45), 503 (46), 536^S (18), 546 (45), 573 (30), 599 (35), 691 (48), 765 (159), 775 (217), 803 (122), 812^S (72), 894 (100)	475$^-$, 603$^-$, 658$^-$, 778$^+$, 788$^-$, 801$^+$, 809$^-$, 818$^+$, 898$^-$
F	471 (27), 505 (29), 539^S (21), 546 (35), 573 (22), 602 (29), 761 (118), 775 (115), 779^S (114), 812 (149), 895 (100)	473$^-$, 604$^-$, 659$^-$, 778$^+$, 787$^-$, 806$^+$, 813$^-$, 819$^+$, 896$^-$

Superscript S denotes shoulders.

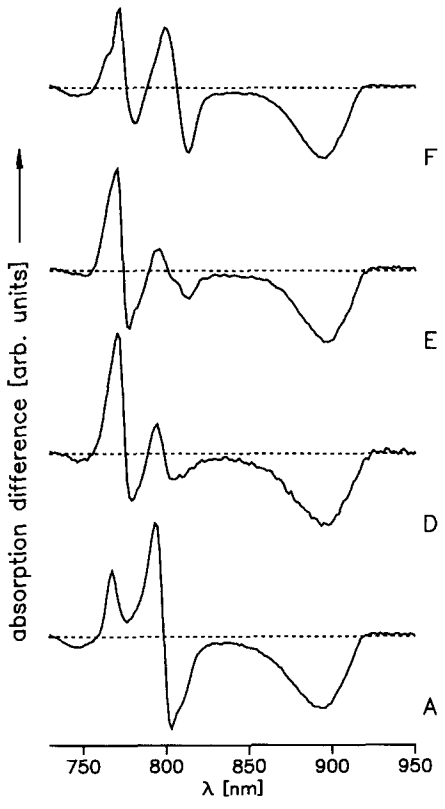

Fig. 3. 'Light-minus-dark' absorption difference spectra of RCs from *Rb. sphaeroides* at ambient K. The spectra are normalized to equal height of the primary donor bleaching band at 896 nm. Notation of the samples is the same as in Fig. 1.

bleaching bands at 804 and 780 nm in addition to enhanced absorption bands at 794 and 771 nm. The preparation modified only at site B_B (sample E) bleaches at 813 and 777 nm and has enhancements at 795 and 770 nm. Finally, the RCs exchanged only at B_A (sample F) exhibit nicely resolved bleaching bands at 814 and 781 nm together with enhanced absorption at 800 and 772 nm with a shoulder at 764 nm.

The ADMR spectrum of the primary donor triplet $^3P_{870}$ of RCs from the 'green' mutant *Rb. sphaeroides* R26, observed on the primary donor absorption band at 890 nm at 8 K, is shown in Fig. 4A. It exhibits three resonance signals at 657 MHz ($|D| + |E|$), 465 MHz ($|D| - |E|$), and 192 MHz ($2|E|$), well known from the literature [33,34]. Since the $2|E|$ signal is weak, it has been amplified by a factor of 10 to be comparable in size with the $|D| \pm |E|$ signals.

Because the ADMR signals of the primary donor triplet of samples B–F are very similar to those of sample A, they were not displayed. The ADMR experiment measures the dipolar interaction between the two unpaired electron spins on $^3P_{870}$. Since neither one of the dimer pigments has been exchanged, D and E stay the same within the error limits of the experiment, yielding similar ADMR spectra when detected on the primary donor absorption. ENDOR experiments performed on the primary donor cation in modified RCs also did not show any substantial change in spin distribution compared to the natural system [35].

The ADMR spectra of the carotenoid triplet states in these samples are shown in Fig. 4. They were recorded on the triplet-triplet absorption band of spheroidene at 550 nm (see legend of Fig. 4). A general feature of these ADMR signals is the relatively strong $2|E|$ signal, appearing between 266 (sample D) and 275 MHz (sample B). The broad $|D| + |E|$ signals appear with two maxima at 980 and 1070 MHz. In samples B and C the splitting of the $|D| + |E|$ signal is especially well resolved. In samples D–F, the lower signal-to-noise ratio obscures the transition and renders the splitting less visible. The intensity ratio between the two $|D| + |E|$ peaks varies from sample to sample and even in the same sample between different freezing cycles [36]. The $|D| - |E|$ signals which are expected between 700 and 800 MHz are either not observed at all or just barely visible, like the extremely weak band at 780 MHz in trace 4C. Upon raising the temperature the two $|D| + |E|$ signals merge to one broad unresolved structure with its maximum around 1000 MHz (not shown) [36]. A similar splitting of the carotenoid triplet signals at

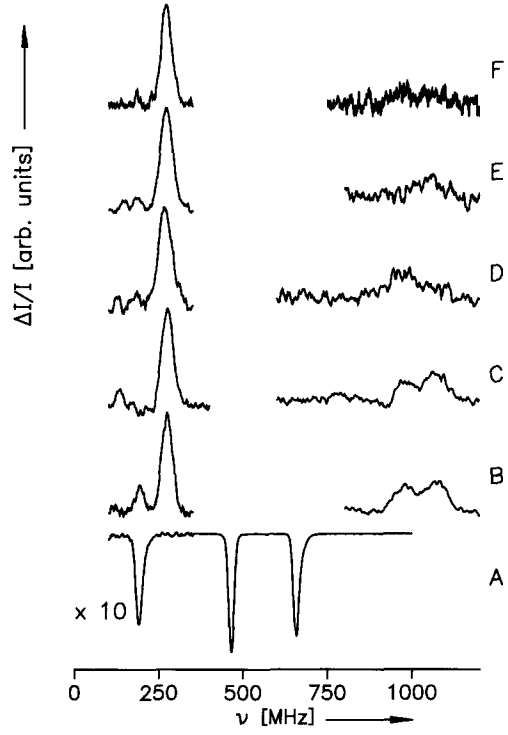

Fig. 4. ADMR spectra of RCs from *Rb. sphaeroides* at 8 K. Notation of the samples is the same as in Fig. 1. (A) RCs of *Rb. sphaeroides* R26 (without carotenoids). The spectrum is the well-known $^3P_{870}$ ADMR spectrum, taken at a detection wavelength of 895 nm. The low frequency part of the spectrum with the $2|E|$ signal has been enhanced by a factor of 10. (B–F) ADMR spectra of the spheroidene triplet state in carotenoid-containing samples B–F, monitored on the triplet-triplet absorption band at 550 nm. All spectra were normalized to equal height at the 270 MHz $2|E|$ signal.

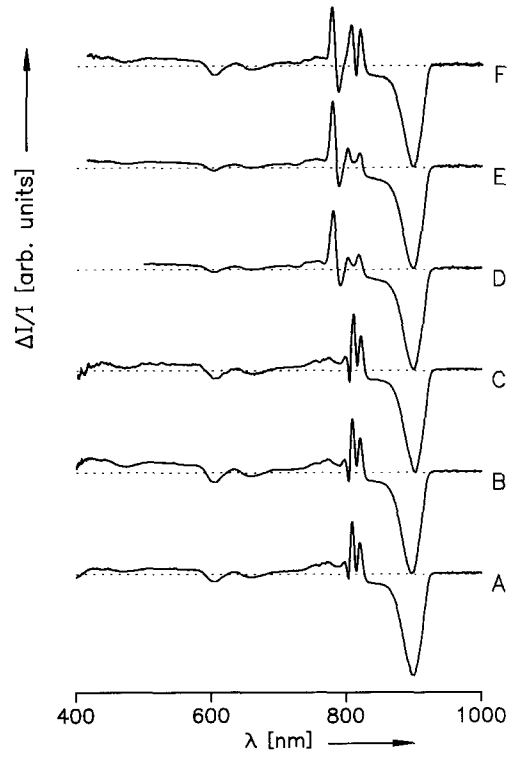

Fig. 5. MIA spectra of RCs from *Rb. sphaeroides* at 8 K between 400 and 1000 nm. The RF frequency was tuned to the maximum of the |D|−|E| transition of the primary donor triplet at 468 MHz. All spectra were normalized to equal height at the red-most bleaching band. The notation for the different samples is as in Fig. 1.

low temperatures has been observed in deuterated preparations by X-band EPR, and was rationalized by two slightly different carotenoid configurations that freeze out at very low temperatures [37,38].

The observation of carotenoid triplet states in the reconstituted RCs demonstrates their functionality as triplet quenchers in the modified and/or spheroidene-reconstituted samples C–F. The similarity of their carotenoid ADMR spectra with those of the native wild-type RC (sample B) demonstrates that the carotenoid (re)constitution was successfully performed in all cases (samples C–E), and that the BChl modifications at site B_A or B_B did not principally interrupt triplet energy transfer to the carotenoid (see below).

The MIA spectra of the primary donor triplet $^3P_{870}$ are shown in Fig. 5 (for band positions see Table 2). MIA spectra are selective T − S (triplet-minus-singlet) absorption difference spectra of only those pigments out of an inhomogeneous distribution that are excited by the RF in resonance with one of their triplet sublevel transitions. The MIA of RCs of *Rb. sphaeroides* R26 was first reported by den Blanken et al. [39]. Our corresponding spectrum 5A (A in Fig. 5) and those of samples B and C are practically identical to those published. The main features are the primary donor absorption bleaching at 896 nm and 604 nm, two narrow positive bands at 820 and 809 nm, and a broad positive offset through most of the visible range which stems from the BChl triplet-triplet absorption. The weak bands between 750 and 790 nm are probably due to the vibronic progression of the bleachings and enhancements of the various Q_y bands of the pigments involved in the formation of the triplet state, but could also reflect some very weak interactions between the primary donor triplet and the two monomeric BChl or the BPh pigments. Additional weak and broad negative bands (singlet-singlet absorption bleachings) are seen in the visible region at 473 and 658 nm. They are probably due to excitonic components of the B_x and Q_x transitions of the dimer constituents.

The fact that both wild-type RCs and those reconstituted with spheroidene exhibit the same $^3P_{870}$ ADMR and MIA spectra as *Rb. sphaeroides* R26 demonstrates that the presence of spheroidene does not directly affect the triplet state on the primary donor, at least not to the extent of visible changes in its triplet-minus-singlet spectra and zero field splittings. We observe the primary donor triplet state because triplet energy transfer $^3P^*_{870} + Car \rightarrow P_{870} + {}^3Car^*$ is thermally activated [40] and switched off at low temperatures.

However, the carotenoid triplet state is observed even at very low temperatures in addition to $^3P_{870}$ in all carotenoid-containing samples (B–F), indicating that at low temperatures a second population mechanism for the carotenoid triplet state is active, as reported earlier [41].

Samples D–F, where either one or both BChl monomers have been replaced by [3-vinyl]-13^2-OH-BChl, show $^3P_{870}$ MIA spectra quite distinct from those of samples A–C. In contrast to the ADMR experiment the MIA spectra show differences in optical transitions on a wavelength scale. These spectra are therefore much more sensitive to pigment modification even if it does not involve the triplet-carrying molecule itself.

Although the main negative bleaching bands of the primary donor at 898 and 604 nm are conserved, the bands in the spectral region around 800 nm have changed drastically. In samples D and E two weak positive bands appear at 818 nm and 802 nm (801 nm for sample E). The trough between these bands is found at 809 nm. Further to the blue we find a negative signal at 790 nm (788 nm for sample E) and a strong positive band with its maximum at 779 nm (778 nm for sample E). The weak bleaching bands in the visible range appear at about the same wavelengths as in the RCs with the native pigments. The MIA spectrum of sample F resembles those of samples D and E, with some differences in the 800 nm region. The two positive bands are closer to each other at 819 and 806 nm and 2–3 times more intense. The minimum separating them is located at 813 nm. The negative and positive bands arising from the modified pigment are located at 787 and 778 nm, respectively.

The MIA spectra of the carotenoid triplet states are shown in Fig. 6. The spheroidene triplet-triplet absorption

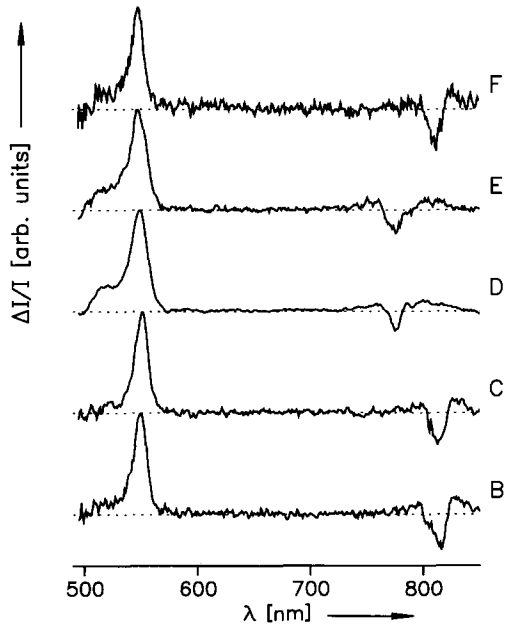

Fig. 6. MIA spectra of RCs from *Rb. sphaeroides* between 500 and 860 nm. The RF frequency was tuned to the maximum of the 2|E| signal of the carotenoid triplet at 270 MHz. All spectra were normalized to equal height at the triplet-triplet absorption band around 550 nm. The notation for the different samples is as in Fig. 1. The sample temperature was set to 8 K for samples, B, C and F, and to 130 K for samples D and E because of sensitivity reasons (samples D and E show a different temperature dependence of their ^{3}Car ADMR signals, yielding appreciably more signal intensity around 130 K than at 8 K in contrast to samples B, D and F).

maximum appears at 550 nm as a positive band. In samples D and E a shoulder around 515 nm is visible which is not as prominent in the other cases. The spectra of samples D and E have been taken at a temperature of 130 K where the ^{3}Car ADMR signals are stronger than at very low temperatures due to a higher thermal activation energy for triplet energy transfer from $^3P_{870}$ through [3-vinyl]-13^2-OH-BChl as compared to the native BChl [42]. In the case of the other samples (with the native BChl at the B_B-site), the temperature dependence of the ADMR signals is quite different, giving good signal intensities already at low temperatures [43].

In the near IR a narrow negative band is found in all samples, superimposed on a broader positive one. It appears at 813 nm in the case of the RCs with native pigments (samples B and C), and in sample F where BChl *a* has been replaced only at site B_A. In samples D and E where either the BChls of the B- or both monomer-sites have been replaced by [3-vinyl]-13^2-OH-BChl, the bleaching appears centred at 776 nm, the absorption maximum of [3-vinyl]-13^2-OH-BChl in the exchanged preparations (see above). This is indicative of an interaction of ^{3}Car with the BChl monomer at the B-side which absorbs at 813 or 775 nm, depending on whether it consists of the natural or the modified pigment.

4. Discussion

The spectra shown in the preceding section will be discussed in terms of changes due to pigment exchange and what they reveal about the contributions of the monomer BChls to the overall RC absorption and MIA spectra. The discussion will also include the effects of pigment–pigment interaction on the MIA spectra, especially for the BChl in the B-site with its nearest neighbours, the primary donor and the carotenoid.

4.1. Spectral changes upon pigment modification

From a detailed analysis of the absorption spectra with selectively modified monomer pigments, the in vivo spectra of the monomer BChls can be deduced and the position of the upper exciton component of the primary donor estimated.

Caution has to be taken, however, since in the RC samples with modified pigments, pigment exchange is not 100% (see Section 2). In particular, the two different monomer sites have different affinities for pigment exchange [22]. The exchange rate of B_B is higher than that of B_A which may result in a mixture of RCs with different numbers of modified pigments, especially in the case of multi-exchange experiments. Thus a 95% replacement of monomeric BChl in sample D may be composed of a 100% exchange at the B_B pocket and a 90% exchange at the B_A pocket. The selective exchange at the B_A site (sample F and the re-exchange experiment of sample E) can be quantified with less uncertainty. The protein pocket of B_B is locked by the presence of spheroidene, thus prohibiting the exchange of B_B. Any loss of the carotenoid during the exchange experiment would principally enable exchange at the B_B site. However, the higher temperatures necessary for pigment exchange in the carotenoid containing RCs will immediately destroy centres which have lost their carotenoid. They are then removed from the sample by the subsequent purification steps and will not contribute to the spectra [44].

Another problem may arise from imperfect reduction of the RCs. We used ascorbate and light to reduce the RCs in all cases. This rather mild method (as compared to dithionite) may result in less than 100% reduction which in turn will affect the relative intensity of the primary donor absorption in the ground state absorption spectra. It is therefore not possible to compare the absorption spectra directly (i.e., to calculate the difference spectrum). Additionally, the freezing conditions of the matrix (a buffer/glycerol 40:60 mixture in all cases) affect the absorption spectra. In those cases where a lot of matrix cracking occurs, the baseline is tilted because of additional scattering in the blue part of the spectrum.

Comparison of the difference spectra is easier. Many of the aforementioned effects do not influence the MIA because they are absorption difference spectra. Varying re-

duction states of the sample will neither pose a problem in ADMR nor in MIA spectra, because one observes only the reduced RCs. Sample inhomogeneities will certainly be observed, at least those due to different degrees of pigment exchange. Since pigment modification of the monomers does not change the primary donor triplet sublevel transitions we can not distinguish RCs with modified monomers from those with native pigments by their ADMR frequencies. All modifications will equally well show up in the MIA spectra according to their concentration in the sample. This is not the case when we monitor the carotenoid triplet MIA. There only those RCs will be detected that actually contain a functional carotenoid pigment.

With these precautions in mind we will now proceed with the discussion of the spectral features of the modified RC complexes and start with the absorption spectra.

4.1.1. The absorption bands of the BChl monomers

Using the selectively exchanged RCs (samples D–F) it is possible to determine the wavelength of the absorption maxima of the A- and B-branch monomers (B_A and B_B, respectively). When native BChl *a* is re-exchanged into the A-branch protein pocket in carotenoid reconstituted RCs with [3-vinyl]-13^2-OH-BChl *a* (sample E), we find an absorbance increase at 803 nm. It indicates that B_A has its Q_y maximum at this wavelength.

On the other hand, when we exchange the A-side monomer against [3-vinyl]-13^2-OH-BChl *a* and leave the native pigment at the B-branch unchanged (sample F), we observe the remaining absorption maximum at 812 nm, which thus can be assigned to the Q_y transition of B_B.

Our assignment is further strengthened by the bleaching band in the MIA spectra of the spheroidene triplet (see Fig. 6, spectra B, C, and F). The bleaching is obviously due to a strong interaction between the triplet state on the carotenoid and the neighbouring BChl monomer, as will be discussed below. Since the A-side monomer is quite far away from the carotenoid this interaction is limited to the B-side monomer, which is again proven by the corresponding MIA spectra where the bleaching is blue-shifted only when the B-side monomer has been modified (see Fig. 6, spectra D and E). The bleaching occurs at 813 nm when native BChl *a* is present at the B-side.

The assignment of the monomer Q_y bands is furthermore supported by the 'light-minus-dark' difference spectra of the different samples. When both monomers are exchanged (see Fig. 3D) the S-shaped feature arising from a band-shift of the monomers (from 803 to 794 nm in *Rb. sphaeroides* R26) is blue-shifted. It now appears at 780 to 771 nm, corresponding to a blue-shift of the [3-vinyl]-13^2-OH-BChl *a* Q_y transition. Upon exchange of the B_A-site only (sample F) the main blue-shift (of the remaining native BChl *a* at B_B) appears from 813 to 800 nm. Our assignment is in good agreement with results obtained by Breton et al. [45] from LD measurements and by Zhou et al. [46] from BPh photoreduction.

Similarly, the Q_x absorption bands of $B_{A,B}$ were located at about 595 and 600 nm for B_A and B_B, respectively. The overlap of the primary donor Q_x band (at 603 nm) makes an accurate distinction rather difficult, however. The modified monomers both absorb at 573 nm and show no difference in peak wavelengths. The difference in absorption maxima for [3-vinyl]-13^2-OH-BChl *a* at sites B_A and B_B is only very small. The corresponding bands in samples D–F appear at 777 and 775 nm, respectively. This indicates that the larger gap and the reversal in ordering of the S_1 energy levels of B_A and B_B in the natural system results from a specific interaction of the 3-acetyl group of the natural BChl *a* with its environment. This specific interaction may at least in part be due to the type of carotenoid present in the complex. The Q_y-band of B_B in *Rhodospirillum rubrum* containing spirilloxanthin as well as in spirilloxanthin-reconstituted RCs from *Rb. sphaeroides* R26 appears at 805 nm, much closer to B_A than if spheroidene or no carotenoid at all is present [23,47,48].

4.1.2. The upper exciton component of P_{870}

Ever since the 'special pair' concept of the primary donor in photosynthetic RCs was introduced [8] attempts were made to determine the exact spectral location of the 'upper exciton component' P_+, which is predicted from the molecular exciton model [49] of two interacting pigments.

From spectroscopic data obtained with circular dichroism and linear dichroism of oriented and non-oriented RC samples, P_+ was assigned to lie within 809 and 815 nm where a slight shoulder in the absorption spectra at low temperatures is visible (see Fig. 1, spectra A–C) [32,45, 48,50–57].

In contrast to this assignment, photoselection measurements and picosecond dichroism data, as well as polarized absorption spectra of single crystals seemed to imply that the upper exciton component has its maximum at 805 nm, well hidden under the 802 nm absorption band, and that the monomer BChl Q_y bands absorb near 802 and 812 nm [58–62].

Other early assignments putting the upper exciton component far below 800 nm [63] or assuming a special trimeric exciton interaction [64] should be mentioned, but seem to be outdated.

It seems that our sample D is well suited to remove this discrepancy in the literature since both monomeric BChl molecules have been replaced by [3-vinyl]-13^2-OH-BChl *a* absorbing about 25 nm to the blue and thus 'lifting the veil' from the upper exciton component. Although there is still a small peak visible at 804 nm which is probably due to incomplete exchange at the A-side, the main absorption band is centred around 807 nm which therefore has to be assigned to the maximum of the upper exciton component of the special pair (see also the simulation of the absorption spectrum in Section 4.1.3).

Given the different affinities of both monomer sites for pigment exchange [22], we can assume that almost 100% of the more readily exchanged B-side monomer have been modified to [3-vinyl]-13^2-OH-BChl *a*. In the absorption spectrum (1D) the remaining 10% native BChl at the A-side at 803 nm is overlapping with the upper exciton component of the primary donor at 807 nm; the exact centre of the peak is therefore not easily determined. Conservatively, we would then put the maximum wavelength of P_+ absorption between 805 and 810 nm.

This assignment assumes that there are no bandshifts due to the pigment exchange, neither induced by structural changes nor by modified pigment–pigment interaction. Since neither the absorption (this paper) nor the CD-bands [18] of the lower exciton band are significantly affected, this assumption seems to be valid (see also Discussion in [19]).

4.1.3. Simulation of the NIR absorption of the doubly-exchanged sample D

Spectral simulations of complex lineshapes using many free parameters (e.g., of a number of Gaussian lines) always carry ambiguities. The simulations shown in Fig. 7 are therefore not meant to actually unravel the many different BChl monomer and dimer transitions and their respective interactions. That would require more elaborate models of pigment–pigment interaction between the various RC co-factors [65–85] and is beyond the scope of this contribution. We regard our spectral simulations simply as a guide for an ad hoc interpretation. It is therefore restricted to the simulation of the spectra of only sample D in the NIR wavelength range above 750 nm. Since this sample has a very high percentage of monomer exchange ($\simeq$ 95% of total monomer content) it gives a direct view of the upper exciton component of the primary donor.

Fig. 7a shows the results of a spectral simulation of the NIR absorption spectrum of sample D between 10 500 and 13 500 cm^{-1}. We used six Gaussian bands to model the part above 12 000 cm^{-1}. The remaining part below 12 000 cm^{-1} consists mainly of the primary donor lower exciton band P_- exhibiting a very asymmetrical band shape with a shoulder at the low-frequency side and a 'pedestal' at the high frequency side (the latter being due to strong electron–phonon interaction). This band has been simulated

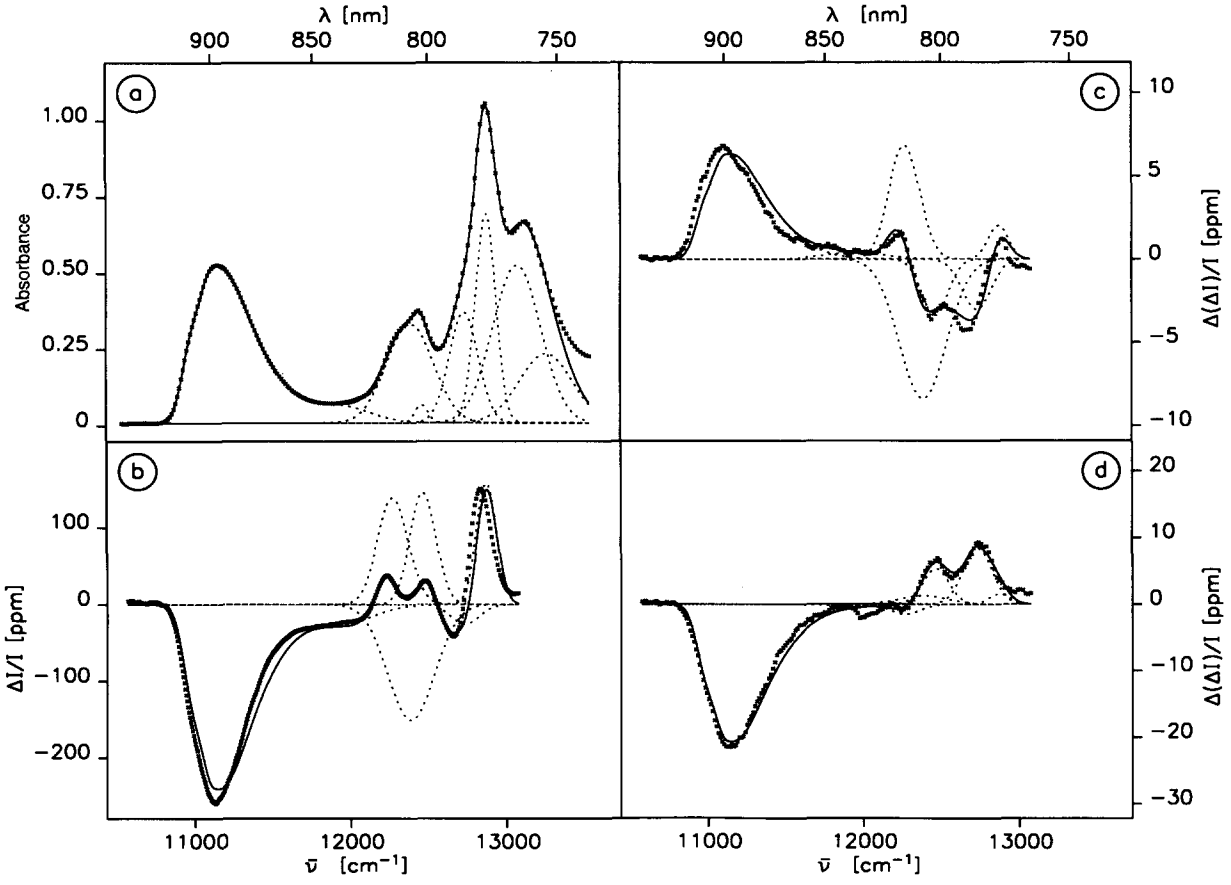

Fig. 7. Spectral simulations of the absorption (a) and MIA (b) spectra of sample D (see Fig. 1D and 5D), and the |D| + |E| (c) and |D| − |E| (d) LD-MIA spectra of the fully exchanged ($B_{A,B}$ modified, but not reconstituted with spheroidene) sample (data taken from [88]). The experimental data are displayed pointwise (×). The individual Gaussian lines used in the simulation (see text and Table 3) are displayed with broken lines (– – –). The sum of all Gaussians gives the simulation curve (–). For the various assumptions concerning the fits, see text.

separately with 4 Gaussians (details not given in Fig. 7a). A good fit was obtained with the parameters given in Table 3 (lines 7–10).

In the spectroscopic range of the monomer Q_y bands (above 12700 cm^{-1}) we need four Gaussian lines to model the RC spectrum which consists of the overlapping bands of the two BPh $H_{A,B}$, and the two monomer BChl molecules ([3-vinyl]-13^2-OH-BChl *a* absorbing around 777 nm) (Gaussians 3 to 6). The range between 12000 and 12700 cm^{-1} contains the absorption bands of the primary donor upper exciton band P_+ (Gaussian 1) and the remaining 5% of non-exchanged native BChl (probably mainly in the B_A-site of the RC, see above) (Gaussian 2).

According to this simulation the maximum of the upper exciton component is located at 807 nm. However, one has to be very cautious, since other possible fits putting the band anywhere between 805 and 810 nm also give reasonable results. Our assignment of P_+ is further supported by a principal component analysis of the absorption spectra of samples D and E by which the contribution of the non-modified RC impurities can be further suppressed mathematically, and which shows a symmetric band centred around 807 nm (data not shown).

The lines derived from this simulation are used without further change of line position or width in the spectral simulation of the MIA-spectra (see Section 4.2.3).

4.2. Spectral decomposition of the $^3P_{870}$ MIA spectra

Given the results of the preceding paragraph we now attempt to decompose the different MIA spectra of the primary donor triplet $^3P_{870}$. As already mentioned, the MIA spectrum is a selective triplet-minus-singlet (T − S) absorption difference spectrum; selective in the sense that only the T − S spectrum of those RCs directly excited by the fixed RF frequency in one of their three triplet sublevel transitions is recorded. This means firstly, that from the inhomogeneous distribution of RC triplets only those are selected that are in resonance. It means secondly, that only that part of the total absorption of these RCs is recorded which is influenced by the triplet generation process; under the conditions stated in the caption of Fig. 5 this is primarily the special pair. The sign of an ADMR or MIA signal is a complex function of the triplet sublevel population and depopulation kinetics, and may thus be positive or negative. In the case of the bacterial RC the 2|E| and

Table 3
Parameters for the spectral simulation of absorption, MIA, and both LD-MIA spectra (|D| ± |E|-transitions) of sample D

	Gaussian	Centre [cm^{-1}] ([nm])	Width [cm^{-1}]	Amplitude [a]
Absorption	1	12384 (807)	210	0.327
	2	12457 (803)	58	0.060
	3	12728 (786)	131	0.365
	4	12868 (777)	92	0.692
	5	13068 (765)	216	0.522
	6	13253 (755)	239	0.217
P_- part	7	10966 (912)	78	0.132
	8	11117 (900)	132 [b]	0.429
	9	11181 (894)	180	0.097
	10	11946 (837)	278	0.051
MIA	1	12384 (807)	210	−0.327 (−100%)
	3	12728 (786)	131	−0.055 (−15%)
	4	12868 (777)	92	0.342 (49%)
	11	12267 (815)	137	0.300 (100%)
	12	12460 (803)	117	0.315 (100%)
LD-MIA (|D| + |E|)	1	12384 (807)	210	0.690 (211%)
	3	12728 (786)	131	−0.249 (−68%)
	4	12868 (777)	92	0.167 (24%)
	11	12267 (815)	137	0.561 (187%)
	12	12460 (803)	117	−0.279 (−89%)
LD-MIA (|D| − |E|)	1	12384 (807)	210	0.032 (9.7%)
	3	12728 (786)	131	0.212 (58%)
	4	12868 (777)	92	0.019 (5.5%)
	11	12267 (815)	137	−0.038 (−13%)
	12	12460 (803)	117	0.133 (42%)

The LD-MIA spectra are actually of the 'green' version of sample D, i.e., prior to spheroidene reconstitution)

[a] Relative intensities of the bands with respect to the absorption bands are given in parentheses. Normalization of the absorption, MIA, and LD-MIA spectral intensities was done on the P_- lower exciton band of the dimer (sum over Gaussians 7–10). P_- is negative in the MIA and the |D| − |E| LD-MIA spectrum.

[b] Asymmetric Gaussian with a line width asymmetry parameter of 3.1.

|D| ± |E| signals all have negative signs if the normalized transmission change upon RF irradiation is displayed [28,39].

In the MIA spectra of all samples A–F we thus observe the lower exciton component of the primary donor as a bleaching around 900 nm. The concomitant bleaching of the upper exciton component around 807 nm, which should also be observed, is obscured by other features indicative of the breaking of excitonic interaction within the dimer upon triplet formation and/or additional interactions between the triplet state on the primary donor and the accessory monomer pigments.

The 800–830 nm range of the MIA spectra of unmodified RCs has been explained earlier by the appearance of a new band around 807 to 809 nm upon triplet formation, the red-shift of a monomer band from 813 to 818 nm, and a blue-shift of another monomer band from 803 to 798 nm [39,86,87]. The bleaching of the upper exciton component of $^3P_{870}$ has not been considered strong enough to be included in the spectral features of the MIA spectra [39]. The band around 807 nm was interpreted as being due to the singlet-singlet absorption of one of the two dimer halves being freed from singlet exciton interaction with each other by the triplet state being located on the other half. At higher temperatures this band disappears, probably due to stronger delocalization of the triplet state over both dimer halves [87].

The MIA spectra of RCs with modified pigments can now be used to check this earlier interpretation.

4.2.1. MIA of sample D

The key spectra for the possible involvement of the monomers to the MIA spectra of $^3P_{870}$ are those of samples D and E. If we take the previous interpretation of the MIA spectra of non-modified RCs for given we would expect in sample D (both monomers exchanged) that the bandshifts of the monomers have disappeared leaving only the positive component due to the absorption of the uncoupled dimer half together with the bleaching of P_+ around 807 nm. Instead we find a 'camelback' shaped difference spectrum with two rather weak positive bands at 802 and 818 nm with a trough around 809 nm (see Fig. 5, spectra D and E, and Fig. 7b).

In order to explain these features we have to consider four different possibilities:

(1) One or both positive bands are at least partly due to residual RCs not fully modified with [3-vinyl]-13^2-OH-BChl *a* at the two monomer positions.

(2) The MIA spectrum between 790 and 830 nm is due to the spectral overlap of one positive and rather broad band centred around 810 nm and one negative and narrower band centred around 807 nm. This would then imply that the Q_y singlet-singlet absorption band of the uncoupled dimer half is located at 810 nm and the upper exciton component of $^3P_{870}$ at 807 nm. (3) The MIA spectrum is due to the spectral overlap of 2 positive bands at 803 and 815 nm with a negative band at 807 nm (as shown in Fig. 7b). This would mean that again the upper exciton component of $^3P_{870}$ is located at 807 nm. However, now two positive bands have to be considered for the absorption of the excitonically uncoupled dimer in its triplet state. Such a situation could be envisioned by a hopping process of the triplet excitation between the two dimer halves. This hopping would have to be slow on the optical time scale giving rise to two distinct absorption bands of the two monomers but fast compared to the microwave time scale since a splitting of the triplet state has never been observed in the microwave frequency domain.

(4) Two positive bands at 803 and 815 nm overlap each other to give the MIA spectrum. A negative band is not needed or may be invoked at shorter wavelengths to account for the negative signal at 791 nm.

The first possibility is discarded since the wavelengths of the positive MIA bands in native RCs do not match with those of the positive features in samples D and E. The main positive MIA band of native RCs at 806 nm appears as a weak shoulder in the MIA spectra of RC preparations that have been exchanged to a lesser extent than the present sample D [88], clearly demonstrating the different origin of these bands.

The second and third possibilities are not easily distinguished, although our simulation of the MIA spectrum of sample D using the Gaussian lines of the absorption simulation gave only a good approximation of the data for case 3 (see Fig. 7b). The camelback feature may in principle be simulated by just two Gaussian lineshapes, one positive and the other negative. However, when using the Gaussians used to fit the absorption spectrum, the remaining triplet-triplet absorption still shows two peaks that can not be fit by a single Gaussian line.

A different view of the matter is to put the upper exciton component at a wavelength of about 790 nm leaving the part between 800 and 820 without a bleaching (possibility 4). Although this could explain the MIA and the LD-MIA spectra of sample D, it does not account for the clearly visible P_+ absorption band at 807 nm in that sample and is therefore dismissed.

4.2.2. Linear dichroism detected ADMR

In order to obtain additional information we consider LD-ADMR (linear dichroism detected ADMR), a method that monitors the polarization of the optical transitions relative to the triplet sublevel transition dipole moments [30]. The selective linear dichroic T − S absorption difference spectra (we call them LD-MIA spectra) used in the spectral simulations (see Fig. 7 and Section 4.2.3) were measured on the fully exchanged RCs, i.e., sample D, prior to spheroidene reconstitution, and were taken from [88]. The difference between that sample and our sample D is only the missing reconstitution with spheroidene.

From the LD-MIA spectra (linear dichroism detected MIA) it is obvious that the transitions giving rise to the

two positive MIA bands at 803 and 815 nm show quite distinct polarization patterns with respect to each other and the primary donor P_- transition. This immediately excludes possibility 2, discussed in the preceding chapter where only two overlapping positive and negative bands make up the MIA spectrum between 790 and 830 nm. In that case the two camelback peaks would be expected to arise from the same transition (triplet-triplet absorption), broader than the overlapping negative (P_+ – bleaching), and to exhibit the same polarization pattern (i.e., same signal sign in the LD-MIA spectrum), which is not observed.

In both LD-MIA spectra the band at 803 nm shows the opposite signal sign compared to that of the P_{870} bleaching. This may be qualitatively interpreted as the Q_y transition of one of the uncoupled dimer halves being polarized more or less parallel to the P_- transition dipole [86]. The band at 815 nm shows the same polarization as the primary donor P_- in the case of the |D| + |E| derived spectrum (see Fig. 7c). For the |D| – |E| derived LD-MIA spectrum this band is too weak to distinguish between positive or negative polarization. Probably, the transition dipole moment is close to the magic angle with respect to the x- and y-directions of the fine structure tensor of $^3P_{870}$ in this case. If one takes the triplet fine structure tensor geometry from the single crystal EPR data by Norris et al. [89] and compares it with the y-directions of the monomeric macrocycles which constitute the dimer, it is clear that Q_y of P_B (B-side dimer half) is closer to the magic angle with respect to $^3P_{870}$ than P_A (A-side dimer half). This would argue for P_B to absorb at 815 nm when the triplet is located on P_A. However, one should keep in mind that the apparent triplet-triplet transition dipole moments of $^1P_A^3P_B^* \rightarrow {}_1P_A^{*3}P_B^*$ and $^3P_A^{*1}P_B \rightarrow {}^3P_A^{*1}P_B^*$ may well experience strong excitonic interaction with each other and even with the BChl monomer pigments $B_{A,B}$. One should therefore not be surprised if their dipole moments do not align with those theoretically expected from the isolated $P_{A,B}$ molecules.

It is instructive to compare our results with the spectral simulations of the MIA spectra of non-modified RCs by Scherer et al. [69,71]. In these calculations based on straightforward exciton theory two triplet-triplet absorption bands of the primary donor special pair are considered in the relevant wavelength region. The wave functions of the excited states to which these transitions lead, are linear combinations of the singlet-singlet excitations of both monomer parts when the triplet state is located on the other half. Scherer et al. place these two bands at 820 and 776 nm for T(+) and T(–), respectively (in the nomenclature used by these authors) [69,71]. The band position at 820 nm lies not too far from our positive MIA band at 815 nm. However, the transition at 776 nm is 27 nm to the blue of our band at 803 nm. It is true that we observe a strong positive band at 777 nm. However, its absence in the MIA spectra of the non-modified RCs clearly shows that it is due to the reconstituted monomeric [3-vinyl]-13^2-OH-BChl *a*.

In principle one has to consider additional exciton interaction between T(±) with the monomer singlet-singlet absorption bands of B_A and B_B [69,71]. This could at least partly explain the increased absorption at 777 nm where the modified monomers absorb, and still leave two distinct absorption bands between 800 and 820 nm with decreased oscillator strengths (oscillator strength is borrowed from the two $^3P_{870}^* \rightarrow$ T(±) transitions by the singlet-singlet absorption of the two [3-vinyl]-13^2-OH-BChl *a* molecules in monomer sites A and B). Whether this is a good explanation for the MIA spectra remains to be shown by theoretical modelling. Furthermore, the assignment of the two bands at 803 and 815 nm to a linear combination of Q_y transitions of the uncoupled P_A and P_B has to be checked by careful quantitative analysis of the microwave power-dependence of the LD-MIA spectra as in [74].

If our above discussion of the two camelback peaks as being due to a linear combination of uncoupled dimer halves is correct, we would expect them to have oscillator strengths comparable to a BChl monomer Q_y absorption band (at least 50% of the P_- bleaching band), more than observed in the bands at 803 and 815 nm. However, we still need to consider the bleaching that is expected from the upper exciton component of the special pair P_+ in the spectral range between 800 and 810 nm. The 'camelback' feature can be modelled if we allow for a negative band at 807 nm due to P_+ bleaching to overlap with these positive features (see Fig. 7b) in agreement with the absorption spectrum of sample D which shows the upper dimer component in this wavelength range. Thereby, the positive bands at 803 and 815 nm gain approximately the expected oscillator strengths.

Although the P_+ bleaching at 807 nm is not directly visible in either of the two LD-MIA spectra, where one would expect it to appear with a polarization opposite to P_-, the spectral simulations (see Section 4.2.3 and Fig. 7c,d) give good fits using the Gaussian bands derived from the absorption and MIA-spectra, including P_+. Since the MIA- as well as the LD-MIA-spectra are more congested in the 800–820 nm range than the optical absorption spectrum even for sample D, it may well be that P_+ is hidden under the triplet-triplet absorption bands in this spectral region.

4.2.3. Simulation of the NIR MIA- and LD-MIA-spectra of sample D

The same caution as in Section 4.1.3 is due when we now proceed with the simulation of the MIA- and LD-MIA-spectra. The simulation relies heavily on the one performed on the absorption spectrum. The obtained fits are mainly supposed to guide the reader through the discussion of the MIA spectral features in the preceding sections.

The simulation of the MIA spectrum of sample D and

the LD-MIA spectra of its carotenoid-free preparation are shown in Fig. 7b–d. We used the Gaussian lines obtained from the fit of the low temperature absorption spectrum without any further change in centre frequency or line width. Since the MIA- and LD-MIA-spectra are somewhat site-selective this leads to simulations that do not completely fit the shape of the primary donor lower exciton band. In these simulations we furthermore neglect the Gaussian lines number 5 and 6. They have to be interpreted as belonging to the BPhe monomers and do not show up in the MIA-spectra. Bands 3 and 4 (see Table 3) probably belong mainly to the modified BChl monomers and are retained in the MIA-spectra. By using their amplitudes as free parameters the part above 12700 cm^{-1} may be fitted reasonably well. In order to simulate the MIA-spectrum between 12000 and 12700 cm^{-1} we need to introduce two more Gaussian lines (numbers 11 and 12 in Table 3) to account for the apparent triplet-triplet absorption due to the breaking of the exciton coupling of the primary donor when the triplet state is located on either one of the dimer halves. Trying to use only one additional Gaussian line did not give a satisfactory fit. Especially the 'camelback' feature can not be reproduced that way.

Similarly, the LD-MIA spectra (see Fig. 7c,d) may be simulated fairly well by just using the Gaussians 1, 3, 4, 11, and 12, in addition to the P_- part of the absorption spectrum by proper adjustment of the respective amplitudes. The polarizations of the lower and upper exciton components are opposite in both LD-MIA simulations, as well as the polarizations of the Q_y transitions of the two dimer halves (apparent triplet-triplet bands, Gaussians 11 and 12), as expected.

4.2.4. MIA bands of the modified monomers

The strong positive band at 779 nm in the MIA spectrum (see Fig. 5D, and at 778 nm in Fig. 5E and 5F) clearly originates from the modified pigments since it is absent in non-modified RCs. The maximum is located slightly to the red of the wavelengths where [3-vinyl]-13^2-OH-BChl *a* shows up in the RC absorption spectrum (see Fig. 1D and E) which seems to exclude a band shift as the only origin of the positive and negative bands at 779 and 790 nm in the MIA spectra. These features are equally strong in the MIA spectra of samples D to F suggesting that the interaction which they are based on are active for both the A- and the B-site monomer. Since the intensities are equal between fully exchanged and partially exchanged RCs one has to admit that the interaction between $^3P_{870}$ and the monomers does not involve both monomers at the same time but is restricted to one at a time. This observation may be rationalized by the assumption of the primary donor triplet state being delocalized over both dimer halves on the time-scale of the ADMR experiment. This would allow for a 'symmetric' interaction of the dimer with both adjacent BChl monomers. In the case of a triplet state localized on only one dimer part one would expect an asymmetric behavior, the interaction being strongest between that part and the monomer BChl closest to it. Earlier findings by Norris and others clearly indicate that the triplet state is delocalized over the special pair in *Rb. sphaeroides* [89,90]. It should be noted at this point that our explanation pertains only to the observation of a symmetric interaction between $^3P_{870}$, and $B_{A,B}$ in the modified RCs. The situation is not so clear-cut in the natural RCs because their MIA spectra are more congested in the wavelength range of interest.

From the 'light-minus-dark' spectra (Fig. 3) the bandshifts of the monomeric BChl pigments upon the formation of the radical pair $P_{870}^+Q_A^-$ can be seen. Native BChl *a* in B_A shows a blue-shift from 803 to 794 nm, in B_B from 814 to 800 nm. [3-Vinyl]-13^2-OH-BChl *a* in B_A exhibits a blue-shift from 781 to 772 nm, and in B_B from 777 to 771 nm.

4.2.5. MIA bands of the monomers in unmodified RCs

Since we have now identified the spectral components in the 800–820 nm region in the modified RCs, and also know the wavelengths of the Q_y-bands of the native BChl *a* monomers in unmodified RCs (see discussion in Section 4.1.1) it should be possible to explain the MIA spectra of unmodified RCs. We assume that there are no extra bandshifts of the upper exciton component and the apparent triplet-triplet absorption due to the modified monomer pigments. As already pointed out in the discussion of the upper exciton component (see Section 4.1.2) the first assumption seems reasonable because we do not observe any considerable bandshift on P_- either, upon monomer exchange. The second assumption may not necessarily hold since the Q_y transitions of the native BChl monomers are energetically very close to the apparent triplet-triplet transitions which stem from the singlet ground state absorption of the uncoupled dimer half when the triplet state is located on its partner. A clearer picture has to await the full theoretical simulation of all the MIA spectra.

Still, we know from the absorption spectra the location of the native monomers and are thus able to assign the sharp features in the MIA spectra of unmodified RCs to bandshifts of these molecules. From inspection of the MIA spectra of samples A to C in Fig. 5, or the difference of the MIA spectra of, e.g., samples D and C (see Fig. 8) it seems obvious that the two BChl *a* monomers experience both a red shift when the primary donor triplet state is populated. The MIA difference of sample D-minus-C (Fig. 8, upper trace) highlights predominantly the effect on the Q_y-bands of the monomers if $^3P_{870}$ is populated. The peak at 779 nm is due to enhanced absorption and possibly a blue-shift from 790 to 779 nm of the [3-vinyl]-13^2-OH-BChl *a* (see preceding section). The two S-shaped features with maxima at 803 and 814 nm and minima at 809 and 819 nm then must be due to band shifts of the native monomers. Obviously, B_A shifts from 803 to 809 nm, whereas B_B shifts from 813 to 819 nm. It is interesting to

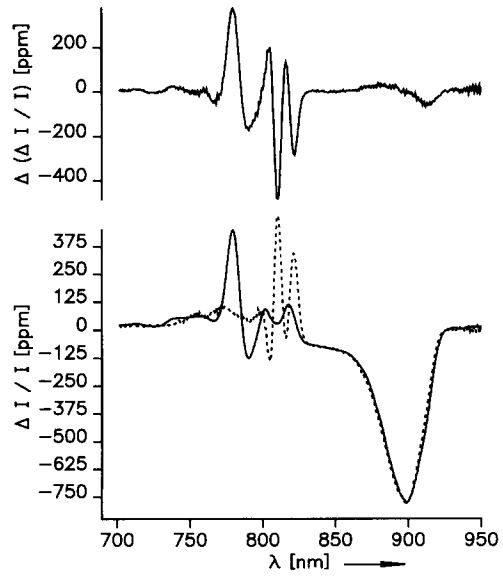

Fig. 8. $^3P_{870}$ MIA spectra of sample D (lower part, –) and of sample C (lower part, – – –), and the resulting difference spectrum (sample D minus C) (upper part) at 8 K.

note that both monomers shift to the red, whereas in the light-minus-dark absorption difference spectrum, where a positive charge is located on the dimer instead of a triplet state, we observe a blue shift of both bands.

Our explanation of the MIA spectrum differs from the one given earlier by Hoff and co-workers [39,86,87] in the following details:

(1) We explain our MIA spectra with a red shift of both monomer Q_y-bands (from 803 to 809 and from 813 to 819 nm) instead of a red shift of the 813 nm band and a blue shift of the 803 nm band, as proposed in [39,86,87].

(2) The bleaching of the upper Davydov component P_+ is masked in the MIA and LD-MIA spectra, which may be the reason why it has been neglected in the earlier assignment of the T − S bands [39,86,87]. From the absorption spectrum of sample D it has to be placed at 807 nm with appreciable oscillator strength.

(3) The apparent triplet-triplet absorption induced by the Q_y transition on the uncoupled dimer half (while the triplet state is residing on the other half) had been assigned to the positive band at 807 nm in the MIA spectra by Hoff et al. [39,86,87]. Considering the small spectral width of this band of only 4 nm at half the maximum height it is much more likely to be part of a band shift than a new BChl monomer Q_y absorption band. In our interpretation it constitutes part of the red shift of B_A from 803 to 809 nm. On the other hand, the apparent triplet-triplet absorption of the uncoupled dimer half exhibits a rather broad double-peak with maxima at 803 and 815 nm (see Fig. 7, and Table 3, bands 11 and 12), which is offset by the P_+ bleaching band at 807 nm.

4.2.6. MIA of sample F

Finally, we want to discuss the MIA spectrum of sample F. It is quite similar to those of samples D and E with some marked differences between 800 and 820 nm. Although the two positive bands are again visible they are about twice as strong and the band maxima are shifted to 806 and 819 nm. The trough between them has become sharper and also more intense and is shifted to 813 nm. In these respects the spectrum resembles more those of unmodified RCs.

If we plot the difference spectrum between the MIA of samples (wild-type) and (wild-type with B_A exchanged against [3-vinyl]-13^2-OH-BChl *a*) (see Fig. 9) we can see the effects of B_A exchange more clearly. Next to a slight shift in the P_- band which may easily be explained by the site-selectivity of the MIA spectra, we find two strong features, resembling band shifts in the Q_y region of the [3-vinyl]-13^2-OH-BChl *a* and native BChl *a* molecules incorporated in the B_A site (see Fig. 9, upper part).

Since the difference spectrum has been calculated by subtracting the MIA of the modified RC preparation (sample F) from that of the non-modified one (sample B), the bandshifts observed have opposite sign. It again shows the red-shift of B_A from 803 to 809 nm for wild-type RCs which is replaced by an absorption increase at 777 nm together with a blue-shift from 790 to 777 nm in the modified RCs.

4.2.7. What can be learnt from the MIA spectra of $^3P_{870}$

In concluding this chapter we want to note the following points that seem to come out fairly well from the MIA spectra:

(1) BChl monomer modification does not strongly affect the triplet state of the primary donor itself. The fine

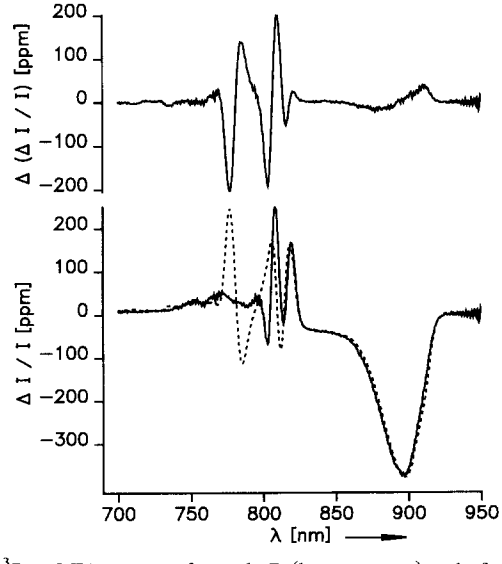

Fig. 9. $^3P_{870}$ MIA spectra of sample B (lower part, –) and of sample F (lower part, – – –), and the resulting difference spectrum (sample B minus F) (upper part) at 8 K.

structure remains the same irrespective of which monomer has been modified. The main bleaching bands of the primary donor in its triplet MIA spectra remain unaffected.

(2) The primary donor triplet state interacts with the monomers on both sides giving rise to red-shifts of $B_{A,B}$ in the MIA spectra between 790 and 830 nm. This is also seen in the bleaching and enhancement at 790 and 777 nm observed in those RCs containing [3-vinyl]-13^2-OH-BChl *a*. The similarity of the MIA spectra of samples D and E is mostly due to incomplete back exchange of native BChl *a* into the B_A-site (sample E), but may also be indicative for a relatively weaker interaction of $^3P_{870}$ with native BChl *a* in B_A. Perhaps, this indicates an asymmetry in the dimer–monomer interaction in the native RCs, similar to the asymmetry observed in the primary electron transfer rates.

(3) The earlier interpretation of the MIA spectrum of non-modified RCs [39,86,87] has to be corrected in some of its details. Two monomer band shifts are observed: B_A experiences a red-shift from 803 to 809 nm; B_B shifts to the red from 813 to 819 nm. For a sufficient description of the MIA bands of fully modified RCs in this region, two apparent triplet-triplet absorption bands at 803 and 815 nm are necessary. They may be described by the linear combination of the two Q_y transitions of the uncoupled dimer parts when the triplet is localized on the respective other half.

(4) The position of the upper exciton component P_+ expected to be visible as a bleaching band in the MIA can not be deduced from the MIA spectra alone. From the absorption spectrum of the fully exchanged RC preparation (sample D) it must be located between 805 and 810 nm. Our spectral simulation puts its centre at 807 nm.

4.3. Interaction between the carotenoid triplet and B_B

We now turn to the interpretation of the carotenoid triplet MIA spectra in Fig. 6. The main features of the MIA spectra of samples B–F are a strong triplet-triplet absorption band around 550 nm with a shoulder around 520 nm and a weaker bleaching band in the near infrared region.

The band at 550 nm belongs to the triplet-triplet absorption of the RC carotenoid spheroidene [91]. The NIR bleaching must, however, be due to the interaction between ^{3}Car and B_B. This is clearly seen by the shift of the band from 813 to 776 nm upon pigment modification at either both monomer sites (sample D) or at site B_B only (sample E). Modification of only B_A (sample F) does not result in a blue shift of the band which is expected since there is no van-der-Waals interaction between the carotenoid and B_A.

An interaction between ^{3}Car and P_{870} has been concluded earlier from magneto-optical difference spectra (MODS), which show a similar somewhat blue-shifted band at 807 nm at higher temperatures in RCs from *Rb. sphaeroides* 2.4.1. It was interpreted as being due to partial delocalisation of the triplet wave function of the carotenoid on B_B [92]. Our spectra agree well with this earlier report, although we observe the bleaching at a longer wavelength, possibly due to the lower temperature our experiment was performed at.

It should be noted that the MIA spectra of ^{3}Car of samples D and E at very low temperatures indeed exhibit some bleaching around 812 nm. These spectra (data not shown) indicate that the pigment exchange is not 100% complete at the B_B-site in both samples.

Nevertheless, the bulk of the RCs in preparations D and E exhibit the ^{3}Car-B_B interaction bands at 776 nm as expected from the preparation which proves that the exchange with the modified pigment was almost complete at least at the B_B site. No bleaching at 776 nm is observed in sample F even at higher temperatures. This proves that the presence of the carotenoid spheroidene in the RC effectively prohibits exchange of B_B. We therefore wish to state that the carotenoid MIA spectra clearly demonstrate the integrity of our preparational approach and thus the validity of the conclusions derived from the experimental results.

5. Conclusions

We have analyzed the absorption and MIA spectra of RCs from *Rb. sphaeroides* R26 with site-specifically modified accessory monomer pigments and reconstituted spheroidene in addition to native and modified RCs from wild-type *Rb. sphaeroides* 2.4.1.

The conclusions drawn from this analysis are the assignments of the Q_y absorption bands of the accessory monomer pigments B_A and B_B at 803 and 812 nm, as well as the assignment of the upper exciton component of the primary donor P_+ in fully exchanged RCs around 807 nm.

The MIA spectra (selective triplet-minus-singlet) of the primary donor triplet where analyzed, based on this information. Between 790 and 820 nm they consist of a red shift of B_A from 803 to 809 nm and a red shift of B_B from 813 to 818 nm. The MIA spectrum of completely exchanged (B_A and B_B) RCs suggests two apparent triplet-triplet absorption bands at 803 and 815 nm due to the uncoupling of exciton interaction in the dimer upon triplet formation in addition to the bleaching of the upper exciton component P_+. The two positive MIA bands are tentatively interpreted as being due to two linear combinations of the singlet-singlet Q_y transitions of the uncoupled dimer part with the respective partner carrying the triplet state. In unmodified or only at B_A modified RCs this splitting may be hidden below other spectral features. Between 770 and 800 nm the interaction of the primary donor triplet with the modified monomer pigments is visible as a bleaching and enhancement of absorption at 790 and 777 nm.

In addition we have demonstrated the specific interaction between B_B and the carotenoid triplet state which may

be explained by a partial delocalization of the carotenoid triplet state wave function on B_B.

Acknowledgements

This work was supported by the Deutsche Forschungsgemeinschaft under contract Wo41/42-2, and SFB 143, project A9. We thank W. Schäfer (Max-Planck-Institute für Biochemie, Martinsried) for providing mass-spectra, and E. Cmiel (Technische Universität München) for NMR spectra of the modified pigments. We also thank C. Bubenzer for growing the bacteria, and I. Katheder for the pigment preparations. G.H. acknowledges a graduate scholarship of the 'Freistaat Bayern'.

References

[1] Reed, D.W. and Peters, G.A. (1972) J. Biol. Chem. 247, 7148–7152.
[2] Straley, S.C., Parson, W.W., Mauzerall, D.C. and Clayton, R.K. (1973) Biochim. Biophys. Acta 305, 597–609.
[3] Feher, G. (1971) Photochem. Photobiol. 14, 373–387.
[4] Okamura, M.Y., Steiner, L.A. and Feher, G. (1974) Biochemistry 13, 1394.
[5] Deisenhofer, J., Epp, O., Miki, K., Huber, R. and Michel, H. (1984) J. Mol. Biol. 180, 385–398.
[6] Chang, C.-H., Tiede, D., Tang, J., Smith, U., Norris, J. and Schiffer, M. (1986) FEBS Lett. 205, 82–86.
[7] Allen, J.P., Feher, G., Yeates, T.O., Komiya, H. and Rees, D.C. (1987) Proc. Natl. Acad. Sci. USA 84, 5730–5734.
[8] Norris, J.R., Uphaus, R.A., Crespi, H.L. and Katz, J.J. (1971) Proc. Natl. Acad. Sci. USA 68, 625–628.
[9] Rockley, M.G., Windsor, M.W., Cogdell, R.J. and Parson, W.W. (1975) Proc. Natl. Acad. Sci. USA 72, 2251–2255.
[10] Clayton, R.K. and Yamamoto, T. (1976) Photochem. Photobiol. 24, 67–70.
[11] Maroti, P., Kirmaier, C., Wraight, C., Holten, D. and Pearlstein, R.M. (1985) Biochim. Biophys. Acta 810, 132–139.
[12] Michel-Beyerle, M.E., Plato, M., Deisenhofer, J., Michel, H., Bixon, M. and Jortner, J. (1988) Biochim. Biophys. Acta 932, 52–70.
[13] Zinth, W., Sander, M., Dobler, J., Kaiser, W. and Michel, H. (1985) in Antennas and Reaction Centers of Photosynthetic Bacteria (Michel-Beyerle, M.-E., ed.), Vol. 42 of Springer Series in Chemical Physics, pp. 97–102, Springer, Berlin.
[14] Coleman, W.J. and Youvan, D.C. (1990) Annu. Rev. Biophys. (Biophys. Chem.) 19, 333–367.
[15] Bylina, E.J. and Youvan, D.C. (1991) in Chlorophylls (Scheer, H., ed.), pp. 705–719, CRC Press, Boca Raton.
[16] Warncke, K. and Dutton, P.L. (1990) in Reaction Centers of Photosynthetic Bacteria (Michel-Beyerle, M.-E., ed.), Vol. 6 of Springer Series in Biophysics, pp. 327–338, Springer, Berlin.
[17] Debus, R.J., Feher, G. and Okamura, M.Y. (1986) Biochemistry 25, 2276–2287.
[18] Struck, A., Cmiel, E., Katheder, I. and Scheer, H. (1990) FEBS Lett. 268, 180–184.
[19] Scheer, H. and Struck, A. (1993) in The Photosynthetic Reaction Center (Deisenhofer, J. and Norris, J.R., eds.), Vol. I, pp. 157–192, Academic Press, San Diego.
[20] DiMagno, T.J., Rosenthal, S.J., Xie, X., Du, M., Chan, C.-K., Hanson, D., Schiffer, M., Norris, J.R. and Fleming, G.R. (1992) in The Photosynthetic Bacterial Reaction Center II. Structure, Spectroscopy, and Dynamics (Breton, J. and Verméglio, A., eds.), Vol. 237 of NATO ASI Series A: Life Sciences, pp. 209–217, Plenum Press, New York.
[21] Finkele, U., Lauterwasser, C., Struck, A., Scheer, H. and Zinth, W. (1992) Proc. Natl. Acad. Sci. USA 89, 9514–9518.
[22] Struck A., Beese, D., Cmiel, E., Fischer, M., Müller, A. and Schäfer, W. (1990) in Reaction Centers of Photosynthetic Bacteria (Michel-Beyerle, M.-E., ed.), Vol. 6 of Springer Series in Biophysics, pp. 313–326, Springer, Berlin.
[23] Müller, A. (1992) Pigmentaustausch und -Einbau in photosynthetischen Reaktionszentren aus *Rhodopseudomonas viridis* und *Rhodobacter sphaeroides*, Ph.D. thesis, Universität München.
[24] Struck, A., Müller, A. and Scheer, H. (1991) Biochim. Biophys. Acta 1060, 262–270.
[25] Feher, G. and Okamura, M.Y. (1978) in The Photosynthetic Bacteria (Clayton, R.K. and Sistrom, W.R., eds.), pp. 349–389, Plenum Press, New York.
[26] Struck, A., Cmiel, E., Katheder, I., Schäfer, W. and Scheer, H. (1992) Biochim. Biophys. Acta 1101, 321–328.
[27] Struck, A. and Scheer, H. (1990) FEBS Lett. 261, 385–388.
[28] Angerhofer, A., Speer, R., Ullrich, J., Von Schütz, J.U. and Wolf, H.C. (1991) Appl. Magn. Res. 2, 203–216.
[29] Angerhofer, A., Friso, G., Giacometti, G.M., Carbonera, D. and Giacometti, G. (1994) Biochim. Biophys. Acta 1188, 35–45.
[30] Den Blanken, H.J., Meiburg, R.F. and Hoff, A.J. (1984) Chem. Phys. Lett. 105, 336–342.
[31] Stollsteimer, H.-U. (1990) Linear-Dichroismus-ADMR an Reaktionszentren photosynthetisierender Bakterien, Diplomarbeit, Universität Stuttgart.
[32] Reed, D.W. and Ke, B. (1973) J. Biol. Chem. 248, 3041–3045.
[33] Clarke, R.H. and Connors, R.E. (1976) Chem. Phys. Lett. 42, 69–72.
[34] Ullrich, J., Angerhofer, A., Von Schütz, J.U. and Wolf, H.C. (1987) Chem. Phys. Lett. 140, 416–420.
[35] Käss, H., Rautter, J., Zweygart, W., Struck, A., Scheer, H. and Lubitz, W. (1994) J. Phys. Chem. 98, 354–363.
[36] Ullrich, J. (1988) Temperaturabhängige ADMR Untersuchungen an Triplettzuständen in den Reaktionszentren photosynthetisierender Bakterien, Ph.D. thesis, Universität Stuttgart.
[37] Kolaczkowski, S.V., Budil, D.B., Bowman, M.K. and Norris, J.R. (1988) Biophys. J. 53, 614a.
[38] Kolaczkowski, S. (1989) On the Mechanism of Triplet Energy Transfer from the Triplet Primary Donor to Spheroidene in Photosynthetic Reaction Centers from *Rhodobacter sphaeroides* 2.4.1, Ph.D. thesis, Brown University.
[39] Den Blanken, H.J. and Hoff, A.J. (1982) Biochim. Biophys. Acta 681, 365–374.
[40] Schenck, C.C., Mathis, P. and Lutz, M. (1984) Photochem. Photobiol. 39, 407–417.
[41] Angerhofer, A., Aust, V., Hofbauer, U. and Wolf, H.C. (1992) in Research in Photosynthesis, Proceedings of the IXth International Congress on Photosynthesis, Nagoya, Japan, August 30–September 4, 1992 (Murata, N., ed.), Vol. 1, pp. 129–132, Kluwer, Dordrecht.
[42] Frank, H.A., Chynwat, V., Hartwich, G., Meyer, M., Katheder, I. and Scheer, H. (1993) Photosyn. Res. 37, 193–203.
[43] Ullrich, J., Speer, R., Greis, J., Von Schütz, J.U., Wolf, H.C. and Cogdell, R.J. (1989) Chem. Phys. Lett. 155, 363–369.
[44] Hartwich, G. (1994), Ph.D. thesis, Technische Universität München.
[45] Breton, J. (1988) in The Photosynthetic Bacterial Reaction Center. Structure and Dynamics (Breton, J. and Verméglio, A., eds.), Vol. 149 of NATO ASI Series A: Life Sciences, pp. 59–69, Plenum Press, New York.
[46] Zhou, Q., Mattioli, T.A. and Robert, B. (1990) in Reaction Centers of Photosynthetic Bacteria (Michel-Beyerle, M.-E., ed.), Vol. 6 of Springer Series in Biophysics, pp. 11–18, Springer, Berlin.
[47] Aust, V. (1995) ADMR und transiente Absorption zum Triplettenergietransfer im bakteriellen Reaktionszentrum, Ph.D. thesis, Universität Stuttgart.

[48] Philipson, K.D. and Sauer, K. (1973) Biochemistry 12, 535–537.
[49] Kasha, M., Rawls, H.R. and El-Bayoumi, M.A. (1965) Pure Appl. Chem. 11, 371–392.
[50] Vermeglio, A. and Clayton, R.K. (1976) Biochim. Biophys. Acta 449, 500–515.
[51] Rafferty, C.N. and Clayton, R.K. (1978) Biochim. Biophys. Acta 502, 51–60.
[52] Rafferty, C.N. and Clayton, R.K. (1979) Biochim. Biophys. Acta 545, 106–121.
[53] Rafferty, C.N. and Clayton, R.K. (1979) Biochim. Biophys. Acta 546, 189–206.
[54] Mar, T. and Gingras, G. (1984) Biochim. Biophys. Acta 764, 86–92.
[55] Breton, J. (1985) Biochim. Biophys. Acta 810, 235–245.
[56] Breton, J., Martin, J.-L., Fleming, G.R. and Lambry, J.-C. (1988) Biochemistry 27, 8276–8284.
[57] Jean, J.M., Chan, C.-K. and Fleming, G.R. (1988) Isr. J. Chem. 28, 169–175.
[58] Vermeglio, A., Breton, J., Paillotin, G. and Cogdell, R. (1978) Biochim. Biophys. Acta 501, 514–530.
[59] Clayton, R.K., Rafferty, C.N. and Vermeglio, A. (1979) Biochim. Biophys. Acta 545, 58–68.
[60] Kirmaier, C., Holten, D. and Parson, W.W. (1983) Biochim. Biophys. Acta 725, 190–202.
[61] Kirmaier, C., Holten, D. and Parson, W.W. (1985) Biochim. Biophys. Acta 810, 49–61.
[62] Frank, H.A., Aldema, M.L., Violette, C.A. and Parot, P.H. (1991) Photochem. Photobiol. 54, 151–155.
[63] Shuvalov, V.A., Asadov, A.A. and Krakhmaleva, I.N. (1977) FEBS Lett. 76, 240–245.
[64] Sauer, K., Dratz, E.A. and Coyne, L. (1968) Proc. Natl. Acad. Sci. USA 61, 17–24.
[65] Knapp, E.W. and Fischer, S.F. (1985) in Antennas and Reaction Centers of Photosynthetic Bacteria (Michel-Beyerle, M.-E., ed.), Vol. 42 of Springer Series in Chemical Physics, pp. 103–108, Springer, Berlin.
[66] Knapp, E.W., Fischer, S.F., Zinth, W., Sander, M., Kaiser, W., Deisenhofer, J. and Michel, H. (1985) Proc. Natl. Acad. Sci. USA 82, 8463–8467.
[67] Vasmel, H., Amesz, J. and Hoff, A.J. (1986) Biochim. Biophys. Acta 852, 159–168.
[68] Knapp, E.W., Scherer, P.O.J. and Fischer, S.F. (1986) Biochim. Biophys. Acta 852, 295–305.
[69] Scherer, P.O.J. and Fischer, S.F. (1987) Biochim. Biophys. Acta 891, 157–164.
[70] Scherer, P.O.J. and Fischer, S.F. (1987) Chem. Phys. Lett. 136, 431–435.
[71] Scherer, P.O.J. and Fischer, S.F. (1987) Chem. Phys. Lett. 137, 32–36.
[72] Warshel, A. and Parson, W.W. (1987) J. Am. Chem. Soc. 109, 6143–6152.
[73] Warshel, A. and Parson, W.W. (1987) J. Am. Chem. Soc. 109, 6152–6163.
[74] Lous, E.J. and Hoff, A.J. (1987) Proc. Natl. Acad. Sci. USA 84, 6147–6151.
[75] Won, Y. and Friesner, R.A. (1988) J. Phys. Chem. 92, 2208–2214.
[76] Parson, W., Warshel, A., Creighton, S. and Norris, J. (1988) in The Photosynthetic Bacterial Reaction Center. Structure and Dynamics (Breton, J. and Verméglio, A., eds.), Vol. 149 of NATO ASI Series A: Life Sciences, pp. 309–317, Plenum Press, New York.
[77] Scherer, P.O.J. and Fischer, S.F. (1988) in The Photosynthetic Bacterial Reaction Center. Structure and Dynamics (Breton, J. and Verméglio, A., eds.), Vol. 149 of NATO ASI Series A: Life Sciences, pp. 319–329, Plenum Press, New York.
[78] Pearlstein, R.M. (1988) in The Photosynthetic Bacterial Reaction Center. Structure and Dynamics (Breton, J. and Verméglio, A., eds.), Vol. 149 of NATO ASI Series A: Life Sciences, pp. 331–339, Plenum Press, New York.
[79] Scherer, P.O.J. and Fischer, S.F. (1989) Chem. Phys. 131, 115–127.
[80] Scherz, A., Fisher, J.R.E. and Braun, P. (1990) in Reaction Centers of Photosynthetic Bacteria (Michel-Beyerle, M.-E., ed.), Vol. 6 of Springer Series in Biophysics, pp. 377–388, Springer, Berlin.
[81] Scherer, P.O.J. and Fischer, S.F. (1991) in Chlorophylls (Scheer, H., ed.), pp. 1079–1093, CRC Press, Boca Raton.
[82] Thompson, M.A., Zerner, M.C. and Fajer, J. (1991) J. Phys. Chem. 95, 5693–5700.
[83] Thompson, M.A. and Zerner, M.C. (1991) J. Am. Chem. Soc. 113, 8210–8215.
[84] Thompson, M.A. and Fajer, J. (1992) J. Phys. Chem. 96, 2933–2935.
[85] Scherer, P.O.J. and Fischer, S.F. (1992) in The Photosynthetic Bacterial Reaction Center II. Structure, Spectroscopy, and Dynamics (Breton, J. and Verméglio, A., eds.), Vol. 237 of NATO ASI Series A: Life Sciences, pp. 193–207, Plenum Press, New York.
[86] Hoff, A.J., Den Blanken, H.J., Vasmel, H. and Meiburg, R.F. (1985) Biochim. Biophys. Acta 806, 389–397.
[87] Lous, E.J. and Hoff, A.J. (1986) Photosyn. Res. 9, 89–101.
[88] Greis, J.W. (1992) Modifizierte Reaktionszentren photosynthetisierender Bakterien - Optisch detektierte magnetische Resonanz, Ph.D. thesis, Universität Stuttgart.
[89] Norris, J.R., Budil, D.E., Gast, P., Chang, C.-H., El-Kabbani, O. and Schiffer, M. (1989) Proc. Natl. Acad. Sci. USA 86, 4335–4339.
[90] Greis, J.W., Angerhofer, A., Norris, J.R., Scheer, H., Struck, A. and Von Schütz, J.U. (1994) J. Chem. Phys. 100, 4820–4827.
[91] Frank, H.A., Chadwick, B.W., Taremi, S., Kolaczkowski, S. and Bowman, M. (1986) FEBS Lett. 203, 157–163.
[92] Lous, E.J. and Hoff, A.J. (1989) Biochim. Biophys. Acta 974, 88–103.